The Photoisomerization of Self-Assembled Monolayers of Azobiphenyls: Simulations Highlight the Role of Packing and Defects.

Valentina Cantatore,[†] Giovanni Granucci,[*,‡] Guillaume Rousseau,[¶] Giancarlo Padula,[‡] and Maurizio Persico[‡]

[†]*Dipartimento di Chimica e Chimica Industriale, Università di Pisa, v. G. Moruzzi 13, I-56124 Pisa, Italy; presently Chalmers*

[‡]*Dipartimento di Chimica e Chimica Industriale, Università di Pisa, v. G. Moruzzi 13, I-56124 Pisa, Italy*

[¶]*Magistère 2 de Physique Fondamentale, Université de Paris Sud 11, Orsay, France*

E-mail: giovanni.granucci@unipi.it

Abstract

We present surface hopping simulations of the photodynamics of SAMs of 4′-(biphenyl-4-ylazo)-biphenyl-4-thiol (ABPT) on Au(111). We show that *trans* → *cis* photoisomerization is suppressed because of steric hindrance in a well ordered SAM. Photoisomerization is instead viable in the presence of defects. Two particularly important defects are the boundaries between domains of *trans*-ABPT molecules leaning in different directions (a line defect) and single *cis* molecules embedded in a SAM of *trans* (a point defect). Our findings explain the cooperative behavior observed during the photoisomerization of a *trans*-ABPT SAM, leading to large domains of pure *cis* and *trans* isomers.[1] The line and point defects are predicted to produce different patterns of *cis*-ABPT molecules during the early stages of the photoconversion.

Keywords

4′-(biphenyl-4-ylazo)-biphenyl-4-thiol - Photoisomerization - Self-assembled monolayers - Surface Hopping

Introduction

Self-assembled monolayers (SAM) of photoswitchable organic compounds allow to modify and control several features of metal surfaces by irradiating with light of suitable wavelengths. The photoisomerization can deeply affect electric conduction, work function, wettability, interaction with living cells, as well as several optical and chemical properties.[2,3,5–12] The azobenzene chromophore is the most frequently used photoswitch, because its *trans* → *cis* and *cis* → *trans* photoisomerizations can be reversibly induced by using light of the appropriate wavelengths, without side reactions, and the two isomers show large differences in structural, electrostatic and optical properties.

SAMs of many different azocompounds were tested, but in several cases the more stable *trans* isomer did not react, or its photoisomerization quantum yield was extremely low.[7,13–22] In many cases the suppression of photoisomerization seems to be correlated with a tight and ordered packing: in fact, effective strategies to improve the photoreactivity are to fabricate mixed SAMs with spacers or to employ azocompounds with large head groups or substituents that decrease density and/or spoil crystalline

order.[7,14,15,20,22] Also the quenching of the excited chromophore due to the proximity of the metal surface can reduce the quantum yields, but this factor should not be important when the chromophores are kept sufficiently far from the surface itself.[23–25] The effect of packing is commonly ascribed to steric hindrance or lack of free volume. In some cases excitonic coupling between neighbouring azobenzene units has been demonstrated,[19,26] but recent simulations indicate that this is not the main cause of low quantum yields.[27]

The case of 4′-(biphenyl-4-ylazo)-biphenyl-4-thiols (azobiphenylthiols, ABPT) depicted in Fig. 1, is particularly interesting. These molecules are non planar because of the typical twisted conformation of the two biphenyl moieties, but are made of two rather long and rigid halves (N-Ph-Ph), so enhancing the steric hindrance opposing photoisomerization. Nevertheless, reversible *trans* → *cis* and *cis* → *trans* photoconversions of SAMs of ABPT and related compounds on Au(111) were performed, with striking effects on the electric conduction and the work function.[1,4,5,9] After a partial *trans* → *cis* conversion, STM images showed that large domains of pure *cis* or pure *trans* isomers were formed, suggesting some kind of cooperative effect.[1]

This paper reports a set of computational simulations of the molecular dynamics for SAMs of ABPT, aimed at clarifying how the photoisomerization occurs in a densely packed SAM. As our main conclusion is that in a well equilibrated and ordered SAM of *trans*-ABPT the photoisomerization is strongly inhibited, we also investigated the role of defects as possible initiators of the process. On the basis of our results, we propose a simple mechanism explaining the formation of domains of pure *trans* and *cis* isomers.

Method and ground state dynamics.

A complete simulation consists of four steps (for more details see the Supporting Information):
(1) A Molecular Dynamics simulation is run in the ground state with periodic boundary conditions, for a duration of 10 ns. The Au(111) surface is represented by four fixed layers of Au atoms. The force field is based on the parameterization by Pipolo et al[33] with some modifications.
(2) A portion of the infinite SAM, corresponding to the unit cell of the MD simulation (96 ABPT molecules for the *trans* isomer, 84 for the *cis* one), is selected for the QM/MM treatment. The azobenzene moiety of one of the central molecules is described by the FOMO-CI semiempirical method,[29–32] to allow for electronic excitation and isomerization (see Fig. 1 for the QM/MM partition). A further equilibration is run for a duration of 50 ps.
(3) The QM molecule is vertically excited to S_1 ($n \rightarrow \pi^*$ band) or to $S_2 - S_4$ ($\pi \rightarrow \pi^*$ band) at randomly chosen phase space points of the QM/MM trajectory, with a further selection based on dipole transition probabilities.
(4) Surface hopping (SH) nonadiabatic trajectories with quantum decoherence corrections[32] are run, starting from the initial conditions of point (3).
The specific features of ABPT, namely two rather long and rigid non-planar rods connected by the azo group, make it a typical case where steric hindrance is more important than electronic excitation transfer between the ABPT molecules and to the metal. The last two effects are neglected in our model, while all other mutual interactions and the vibrational energy transfer within the SAM are taken into account, along with all kinds of conformational effects.

Figure 1: The 4′-(biphenyl-4-ylazo)-biphenyl-4-thiol molecule (ABPT). In the red box, the azobenzene moiety treated at QM level in the simulations of the photodynamics.

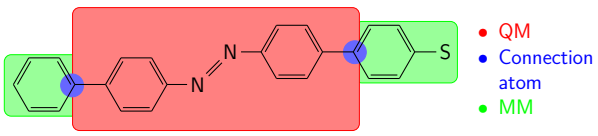

We first considered four kinds of SAM: two made of *trans*- or *cis*-ABPT only (all-*trans* and all-*cis*) and two with one *trans* or *cis* molecule embedded in a SAM of the other isomer (one-*trans* and one-*cis*). All the SAMs are built with

the same ratio of three ABPT molecules every ten Au atoms in the first layer, as found experimentally[1] and by previous simulations.[34] Assuming a first neighbour distance of 2.88 Å between Au atoms, this yields a coverage of 4.17 molecules/nm^2. Preliminary SH simulations of the photodynamics triggered by $n \rightarrow \pi^*$ excitation, run on the basis of shorter MD equilibrations, showed that the *trans* $\rightarrow$ *cis* photoisomerization in the all-*trans* SAM is severely hindered. On the contrary, for the other three envisaged cases the quantum yields were found close to those of azobenzene in usual solvents or in vacuo:[30] namely, in the one-*trans* SAM we obtained the *trans* $\rightarrow$ *cis* quantum yield $\Phi_{t\rightarrow c} \simeq 0.3$, and in both the all-*cis* and the one-*cis* SAMs the *cis* $\rightarrow$ *trans* quantum yield was $\Phi_{c\rightarrow t} \simeq 0.6$. Some tests with $\pi \rightarrow \pi^*$ excitation showed similar results. Therefore, we focussed on the most problematic case of *trans* $\rightarrow$ *cis* photoisomerization in the all-*trans* SAM and left the other cases for a more sistematic investigation.

Figure 2: Snapshot of the unit cell of the all-*trans* SAM. The Au atoms of the upper layer are shown as small dots, the S atoms as larger yellow circles, the lower phenyl rings in blue, the azobenzene moieties in green and the upper phenyl rings in purple.

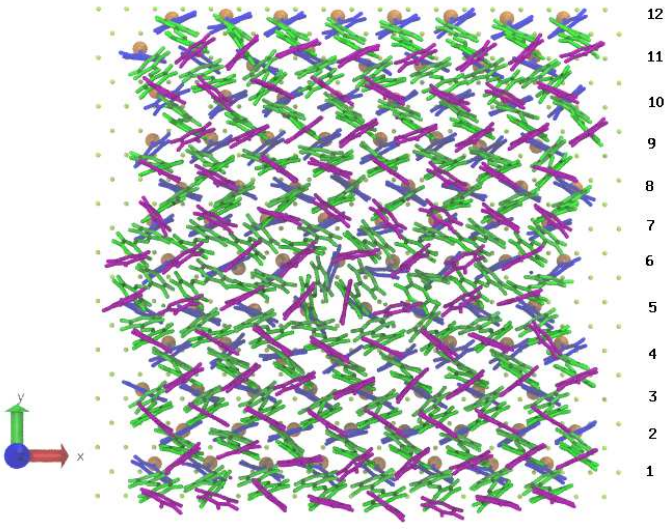

The all-*trans* or all-*cis* SAMs show fairly regular structures (see Figures 2 and S1). The S atoms form straight rows parallel to one of the three equivalent directions of the Au lattice, that we shall take as the x reference axis, z being the perpendicular to the Au surface. Along a row the S atoms are 5.76 Å apart from each other in the average (averages are taken over time and for the whole sample, when not otherwise specified). The mean separation between rows is 4.16 Å. In the all-*trans* SAM the azobenzene moieties are approximately planar, but the phenyl rings at the two ends form angles of approximately 60° with the core ones, as in free biphenyl. The resulting herringbone pattern agrees with the STM images[1] and with previous simulations.[34] The *trans*-ABPT molecules are slightly tilted, i.e. the axis joining the S atom with the farthest C atom forms an angle θ with the z axis, that averages to 13.2° (see Fig. S2). All the ABPT molecules belonging to a given row lean approximately in the same direction, determined by the azimuthal angle ϕ, during the whole simulation (see the ϕ distributions in Fig. S3). The ϕ angle average is in the range $[-90°, -60°]$ for most of the rows, but falls instead in the range $[-135°, -125°]$ for the 6-th, 7-th and 8-th rows (see Fig. 2 for the numbering of rows). The 6-th row also shows the largest tilt angle, about 20° in the average. The pairs of rows 5-6 and 8-9, being at the boundary between two differently oriented zones, experience a less regular packing environment (notice that also the herringbone pattern is disrupted for these row pairs), so may be expected to photoisomerize more easily than others.

Table 1: Energy differences ΔE_{c-t} between the *cis* and *trans* ABPT isomers in different environments (kcal/mol), obtained by force field calculations

molecular system	ΔE_{c-t}
single molecule in vacuo[a]	13.1
all-*cis* vs all-*trans* SAM[b,c]	29.6
one-*cis* vs all-*trans* SAM[b]	15.5
all-*cis* vs one-*trans* SAM[b]	5.9

[a] Equilibrium geometry. [b] Molecular Dynamics, time average. [c] Energy per molecule (the total energy of each SAM is divided by the number of molecules).

Based on the MD simulations we computed the ΔE_{c-t} averaged energy differences between the *cis* and *trans* isomers in different environments (see Table 1). The much larger ΔE_{c-t}

obtained in pure SAMs with respect to the single molecule shows that the *trans* isomer packs much more favorably than the *cis* one. However, converting one *trans* molecule to *cis* within the all-*trans* SAM requires little more energy than in vacuo, while in the all-*cis* SAM it is much easier.

Excited state dynamics and role of defects.

In order to test the hypothesis that the photoisomerization may be easier at the boundary between two regions with different tilt orientation, we simulated the nonadiabatic dynamics by selecting the QM molecule in the "boundary" rows 5 and 6 and in the "normal" rows 3 and 4 of the all-*trans* SAM. We ran a total of 539 SH trajectories starting with $n \rightarrow \pi^*$ excitation and lasting 20 ps. We also ran a simulation for an isolated ABPT molecule, for comparison. The results are shown in Table 2. The $\Phi_{t\rightarrow c}$ quantum yields were computed taking into account only the trajectories that settled at *trans* or *cis* geometries in the ground state within 20 ps. Only the 6-th row showed a small quantum yield, $\Phi_{t\rightarrow c} \simeq 0.087$, while in the other rows no trajectory did isomerize. The $\pi \rightarrow \pi^*$ excitation produced essentially the same results: a quantum yield 0.068 for the 6-th row (typically smaller than the $n \rightarrow \pi^*$ one[35]) and no photoisomerization for the other rows. As seen in the previous section, this photoisomerization is only slightly more endothermic than in vacuo, so the real obstacle must lie along the photoisomerization pathway. Azobenzene has been shown to photoisomerize by torsion of the N=N double bond, even in constraining environments,[30,35–37] and we found the same for the isolated ABPT molecule. The S_0/S_1 crossing seam coincides with the S_1 minimum energy pathway along the torsional coordinate represented by the dihedral angle CNNC, around CNNC=95°. As a consequence, the nonadiabatic transitions to S_0 occur mostly in this region or slightly before (CNNC between 90° and 120°).[30,35] In ABPT, the torsional motion is more easily hindered by the environment, because the two rigid rods N-Ph-Ph require more room to rotate with respect to each other. As a consequence, the torsional motion is delayed and most of the $S_1 \rightarrow S_0$ hops take place at angles closer to 180°, leading to reversion to the initial *trans* structure (see Figs. S4 and S5). A few exceptions occur only when the excited molecule is in the 6-th row. Of course, the nonadiabatic transitions far from the conical intersection region are much slower, so the S_1 lifetime is very long with respect to the isolated molecule, with the 6-th row representing an intermediate case (see Table 2).

Table 2: Quantum yieds $\Phi_{t\rightarrow c}$ and lifetimes τ of the S_1 state for the $n \rightarrow \pi^*$ photodynamics.

environment and position of the excited molecule	number of trajs.	$\Phi_{t\rightarrow c}$	τ (ps)
in vacuo	308	0.33	0.9
all-*trans* SAM, row 3	96	0.0	31.1
all-*trans* SAM, row 4	116	0.0	28.5
all-*trans* SAM, row 5	132	0.0	29.6
all-*trans* SAM, row 6	195	0.087	10.4
one-*cis* SAM, position 1	102	0.059	4.7
one-*cis* SAM, position 2	213	0.110	2.6
one-*cis* SAM, position 3	111	0.022	13.8

The coexistence of two different tilt orientations within the all-*trans* SAM may depend on the way the SAM is assembled and on the equilibration time, both in real experiments and in simulations. For instance, separate domains with different tilt orientations may form before the surface coverage is complete and then expand till they join, leaving seams with unmatched orientations. Our results show that an all-*trans* SAM with a high degree of 2-dimensional crystalline order is not photoreactive. However, defects such as a change in the tilt direction can introduce a (small) photoreactivity, by disrupting the tight packing that hinders the photoisomerization. It is obvious that vacancies may have a similar effect, because of the larger free volume enjoyed by the neighboring molecules. Preliminary MD simulations showed that it is not trivial to determine how many molecules are perturbed by the presence of a vacancy, because even the anchoring of S atoms to the gold surface is affected.

Another interesting kind of defect is the presence of one *cis* molecule in a SAM of *trans*.

We simulated the photoisomerization of *trans* molecules in three locations near the defect: two of them are nearest neighbors of the *cis* molecule (positions 1 and 2 in Fig. 3); the last one (position 3) is a second neighbor, presumably the most affected by the presence of the *cis* molecule which leans just in its direction. We found sizeable quantum yields for positions 1 and 2, and a very small one for position 3 (see Table 2). In the first two cases the lifetimes were much smaller than those of the all-*trans* SAM, even at the 6-th row, showing that the distorsion caused by the *cis* neighbor speeds up the twisting of the N=N double bond, but does not guarantee to achieve the isomerization with a high probability. It is clear that the almost complete inability of *trans*-ABPT to photoisomerize except in the close proximity of a *cis* molecule is the reason for the formation of pure *cis* domains in the early stages of photolysis.[1]

Figure 3: Snapshot of part of the one-*cis* SAM. The colors have the same meaning as in Fig. 2. The numbers mark the three *trans* molecules for which the photoisomerization has been simulated.

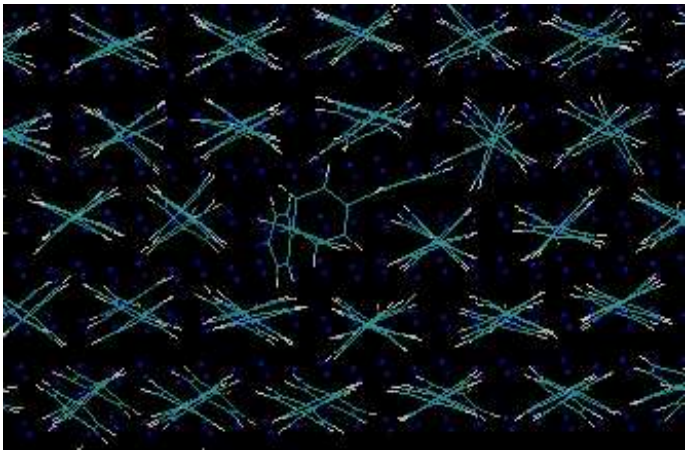

Conclusions.

Surface hopping simulations of the photodynamics of *trans*-azobiphenylthiol in a SAM show that isomerization cannot occur unless some kind of defect perturbs the regularity of packing. The inhibition of photoisomerization is not due to the endothermicity of the reaction, which is not much higher than in vacuo, but rather to steric hindrance that prevents the twisting of the central N=N double bond. The Internal Conversion to the ground state is also delayed. Sufficient free volume for the photoisomerization to occur may be provided by vacancies in the 2D crystalline structure of the SAM. We have shown that photoisomerization also occurs at the boundary between two domains of molecules with different tilt directions (i.e. azimuthal angles), that normally tend to be the same for adjacent rows of molecules.

When a single *cis* molecule is present, we find that its *trans* first neighbors are able to photoisomerize. This behaviour is the key to the cooperative behaviour observed by Pace et al,[1] resulting in large domains of pure *cis* and pure *trans* isomers. This is probably also a factor pushing both the $trans \rightarrow cis$ and the $cis \rightarrow trans$ photoisomerizations towards completeness, a feature of great importance for technological applications.

We predict that experiments with short irradiation times and low intensities would yield different results for the two kinds of defects we have simulated. The boundary between domains with different tilt orientations is expected to yield long strips of *cis* isomers. A *trans*-SAM seeded with few *cis* molecules would instead grow small islands of photoisomerized molecules around each of them. More generally, our results confirm that a careful preparation of a regularly packed SAM of azocompounds can suppress photoisomerization, while short equilibration times or other conditions leading to defective structures are likely to increase the $trans \rightarrow cis$ quantum yields, as several experimental clues already suggested.[1,4,7,13–22]

References

(1) Pace, G.; Ferri, V.; Grave, C.; Elbing, M.; von Hänisch, C.; Zharnikov, M.; Mayor, M.; Rampi, M. A.; Samorì, P. *Proc. Natl. Acad. Sci. USA* **2007**, *104*, 9937.

(2) Browne, W. R.; Feringa, B. L. *Annu. Rev. Phys. Chem.* **2009**, *60*, 407.

(3) Wang, Z.; Nygøard, A.-M.; Cook, M. J.; Russell, D. A. *Langmuir* **2004**, *20*, 5850.

(4) Elbing, M.; Błaszczyk, A.; von Hänisch, C.; Mayor, M.; Ferri, V.; Grave, C.; Rampi, M. A.; Pace, G.; Samorì, P.; Shaporenko, A.; Zharnikov, M. *Adv. Funct. Mater.* **2008**, *18*, 2972.

(5) Ferri, V.; Elbing, M.; Pace, G.; Dickey, M. D.; Zharnikov, M.; Samorì, P.; Mayor, M.; Rampi, M. A. *Angew. Chem. Int. Ed.* **2008**, *47*, 3407.

(6) Smaali, K.; Lenfant, S.; Karpe, S.; Oçafrain, M.; Blanchard, P.; Deresmes, D.; Godey, S.; Rochefort, A.; Roncali, J.; Vuillaume, D.; *ACS Nano* **2010**, *4*, 2411.

(7) Yeung, C. L.; Charlesworth, S.; Iqbal, P.; Bowen, J.; Preeceb, J. A.; Mendes, P. M. *Phys. Chem. Chem. Phys.* **2013**, *15*, 11014-11024.

(8) Joshi, G. K.; Blodgett, K. N.; Muhoberac, B. B.; Johnson, M. A.; Smith, K. A.; Sardar, R. *Nano Lett.* **2014**, *14*, 532.

(9) Merari Masillamani, A.; Osella, S.; Liscio, A.; Fenwick, O.; Reinders, F.; Mayor, M.; Palermo, V.; Cornil, J.; Samorì, P. *Nanoscale* **2014**, *6*, 8969-8977.

(10) Orgiu, E.; Samorì, P. *Adv. Mater.* **2014**, *26*, 1827-1845.

(11) Schulze, M.; Utecht, M.; Moldt, T.; Przyrembel, D.; Gahl, C.; Weinelt, M.; Saalfrank, P.; Tegeder, P. *Phys. Chem. Chem. Phys.* **2015**, *17*, 18079-18086.

(12) Köhntopp, A.; Dittner, M.; Temps, F. *J. Phys. Chem. Lett.* **2016**, *7*, 10881095.

(13) Wang, R.; Iyoda, T.; Jiang, L.; Tryk, D. A.; Hashimoto, K.; Fujishima, A. *J. Electroanal. Chem.* **1997**, *438*, 213.

(14) Evans, S. D.; Johnson, S. R.; Ringsdorf, H.; Williams, L. M.; Wolf, H. *Langmuir* **1998**, *14*, 6436.

(15) Tamada, K.; Akiyama, H.; Wei, T.-X.; Kim, S.-A. *Langmuir* **2003**, *19*, 2306.

(16) Akiyama, H.; Tamada, K.; Nagasawa, J.; Abe, K.; Tamaki, T. *J. Phys. Chem. B* **2003**, *107*, 130.

(17) Weidner, T.; Bretthauer, F.; Ballav, N.; Motschmann, H.; Orendi, H.; Bruhn, C.; Siemeling, U.; Zharnikov, M. *Langmuir* **2008**, *24*, 11691.

(18) Siemeling, U.; Bruhn, C.; Bretthauer, F.; Borg, M.; Träger, F.; Vogel, F.; Azzam, W.; Badin, M.; Strunskus, T.; Wöll, C. *Dalton Trans.* **2009**, , 8593.

(19) Gahl, C.; Schmidt, R.; D, ,; . Brete; E. R.McNellis Freyer, W.; Carley, R.; Reuter, K.; Weinelt, M. *J. Am. Chem. Soc.* **2010**, *132*, 1831. Structure and Excitonic Coupling in Self-Assembled Monolayers of Azobenzene-Functionalized Alkanethiols.

(20) Ishikawa, D.; Ito, E.; Han, M.; Hara, M. *Langmuir* **2013**, *29*, 4622.

(21) Müller, M.; Jung, U.; Gusak, V.; Ulrich, S.; Holz, M.; Herges, R.; Langhammer, C.; Magnussen, O. *Langmuir* **2013**, *29*, 10693.

(22) Valley, D. T.; Onstott, M.; Malyk, S.; Benderskii, A. V. *Langmuir* **2013**, *29*, 11623.

(23) Comstock, M. J.; Levy, N.; Kirakosian, A.; Cho, J.; Lauterwasser, F.; Harvey, J. H.; Strubbe, D. A.; Fréchet, J. M. J.; Trauner, D.; Louie, S. G.; , **F**, *M*, ... CrommiePhys. Rev. Lett.990383012007

(24) Schmidt, R.; Hagen, S.; Brete, D.; Carley, R.; Gahl, C.; Dokić, J.; Saalfrank, P.; Hecht, S.; Tegeder, P.; Weinelt, M. *Phys. Chem. Chem. Phys.* **2010**, *12*, 4488.

(25) Benassi, E.; Corni, S. *J. Phys. Chem. C* **2014**, *118*, 25906-25917.

(26) Utecht, M.; Klamroth, T.; Saalfrank, P. *Phys. Chem. Chem. Phys.* **2011**, *13*, 21608.

(27) Titov, E.; Granucci, G.; Götze, J.; Persico, M.; Saalfrank, P., submitted

(28) Tirosh, E.; Benassi, E.; Pipolo, S.; Mayor, M.; Valášek, M.; Frydman, V.; Corni, S.; Cohen, S. R. *Beilstein J. Nanotechnol.* **2011**, *2*, 834.

(29) Granucci, G.; Persico, M.; Toniolo, A. *J. Chem. Phys.* **2001**, *114*, 10608-10615.

(30) Cusati, T.; Granucci, G.; Persico, M.; Photodynamics and time-resolved fluorescence of azobenzene in solution: a mixed quantum-classical simulation, *J. Am. Chem. Soc.* **2011**, *133*, 5109-5123.

(31) Cusati, T.; Granucci, G.; Martínez-Núñez, E.; Martini, F.; Persico, M.; Vázquez, S., *J. Phys. Chem. A* **2012**, *116*, 98-110.

(32) Granucci, G.; Persico, M. *Theor. Chem. Acc.* **2014**, *133*, 1526-1553.

(33) Pipolo, S.; Benassi, E.; Brancolini, G.; Valášek, M.; Mayor, M.; Corni, S. *Theor. Chem. Acc.* **2012**, *131*, 1274-1283.

(34) Pipolo, S.; Benassi, E.; Corni, S. *Langmuir* **2013**, *29*, 10505-10512.

(35) Cantatore, V.; Granucci, G.; Persico, M. *Comput. Theor. Chem.* **2014**, *1040*, 126-135.

(36) Ciminelli, C.; Granucci, G.; Persico, M. *J. Chem. Phys.* **2005**, *123*, 174317/1-10.

(37) Creatini, L.; Cusati, T.; Granucci, G.; Persico, M. *Chem. Phys.* **2008**, *347*, 492-502.

The Photoisomerization of Self-Assembled Monolayers of Azobiphenyls: Simulations Highlight the Role of Packing and Defects.

V. Cantatore[†], G. Granucci, G. Rousseau[‡], G. Padula, M. Persico

Dipartimento di Chimica e Chimica Industriale, Università di Pisa, v. G. Moruzzi 13, I-56124 Pisa, Italy

[†]*Current address: Department of Chemistry and Chemical Engineering, Energy & Materials, Chalmers University of Technology, Gothenburg, Sweden*

[‡]*Current address: Epitech Paris, 24 rue Pasteur, 94270 Le Kremlin-Bicêtre, France*

SUPPORTING INFORMATION

Computational details.
The MM force field used in our calculations was the OPLS/AA [1] as implemented in TINKER [2]. In particular, the following functional form was used:

$$E_{MM} = \sum_{bond} K_r(R-R_0)^2 + \sum_{angles} K_\alpha(\alpha-\alpha_0)^2 + \sum_{\substack{improp.\\tors.}} K_\delta(\delta-\delta_0)^2 + \sum_{dihed.}\sum_{n=1}^{4}\frac{C_n}{2}[1+\cos(n\delta)]$$
$$+ \sum_{i<j}^{atoms}\frac{q_i q_j}{R_{ij}^2} + \sum_{i<j}^{atoms} 4\epsilon_{ij}\left[\left(\frac{\sigma_{ij}}{R_{ij}}\right)^{12} - \left(\frac{\sigma_{ij}}{R_{ij}}\right)^{6}\right]$$

where the first line describe the bonding interactions, and the second line the non bonding terms. With respect to the OPLS/AA force field, some parameter were modified or added, mainly following the work of Pipolo *et al* [3] for the ABPT molecule and that of Vlugt *et al* [4] for the interaction with the gold atoms: these parameters are shown in Table S1 and S2. The Au atoms were frozen during the dynamics simulations: the Au-Au interactions were therefore not considered.

The MD simulations for the full MM systems where performed with the TINKER program package [2], using periodic boundary conditions. For all the four systems considered (all-*trans*, all-*cis*, one-*trans* and one-*cis*, see the main text) the dynamics were run for a total time of 10 ns at 300 K, with an integration time step of 1 fs. The first part of the MD, showing a drift in the total energy, was eliminated, keeping only the last 6, 3, 6, and 5 ns for all-*trans*, all-*cis*, one-*trans* and one-*cis*, respectively.

The QM/MM calculations were performed with our development version of the MOPAC2002 program [6], connected to TINKER for the treatment of the MM part. The QM moiety (see Figure 1) was described by the FOMO-CI method, using a semiempirical AM1 Hamiltonian reparameterized for azobenzene [7], which has proven to reproduce very accurately experimental and high-level ab initio data for that chromophore. No further reparameterization was attempted in the present case also because the absorption spectra of *trans* and *cis* ABPT are very similar to those of azobenzene [8, 9]. The electrostatic embedding was adopted and the QM-MM link was described using the "connection atom" approach of Antes and Thiel [10, 11]. In the QM/MM dynamics the periodic boundary conditions were not used; for this reason, the motion of selected carbon atoms belonging to the ABPT molecules located on the borders of the slab was restrained by applying a 3D harmonic potential. The QM/MM ground state equilibrations were performed at 300 K with the Bussi Parrinello thermostat

Table S1: MM force field: parameters for bonded interactions. Presented are the parameters added/modified with respect to the standard OPLS/AA force field, as implemented in TINKER [2]. CB labels the "bridge" carbon atoms connecting the two phenyl rings. R_0 in Å, K_r in kcal mol^{-1} Å^{-2}, α_0 in degrees, K_α in kcal mol^{-1} rad^{-2}, C_1-C_4 in kcal mol^{-1}.

bond stretching			R_0	K_r			
N	N		1.2459	1385.1	from ref. [3]		
C	N		1.4124	567.94	from ref. [3]		
angle bending			α_0	K_α			
C	CB	CB	117.271	103.24	from ref. [3]		
C	C	N	119.127	87.204	from ref. [3]		
C	N	N	112.5	89.833			
C	C	S	120.0	70.0			
dihedral				C_1	C_2	C_3	C_4
C	CB	CB	C	0.100	-0.956	0.0167	0.394	from ref. [3]
C	C	N	N	0	-3.5	0	0	
C	N	N	C	0	-40.0	0	0	

Table S2: MM force field: parameters for nonbonded interactions. Presented are the parameters added/modified with respect to the standard OPLS/AA force field, as implemented in TINKER [2]. CB labels the "bridge" carbon atoms connecting the two phenyl rings. CS and CN label the carbon atoms directly linked to S and N, respectively. σ in Å, ϵ in kcal/mol, charges in a.u.

Lennard Jones				
Site		σ	ϵ	
S		4.45	0.25	from ref. [4]
CS		3.50	0.066	
Pair		σ	ϵ	
S	Au	2.400	8.4650	from ref. [4]
CS	Au	3.365	0.1373	
C	Au	3.173	0.0640	from ref. [5]
H	Au	2.746	0.0414	from ref. [5]
N	Au	3.225	0.1630	

Electrostatic		
Atom	Charge	
N	-0.25	from ref. [3]
CN	0.25	from ref. [3]
CB	0.0	from ref. [3]
CS	0.18	
S	-0.18	

[12], starting from geometries sampled from the MD simulations referred above and using a time step of 0.1 fs. The same integration time step of 0.1 fs was also employed in the QM/MM surface hopping nonadiabatic dynamics simulations (both for the nuclear and for the electronic degrees of freedom). The quantum decoherence was approximately taken into account using our energy based correction (EDC), with $C = 1.0$ hartree [13].

Figure S1: Snapshot of the unit cell of the all-*trans* SAM, side view. The Au atoms are shown as dots, the S atoms are larger yellow circles. The 12 rows of ABPT molecules are clearly distinguishable.

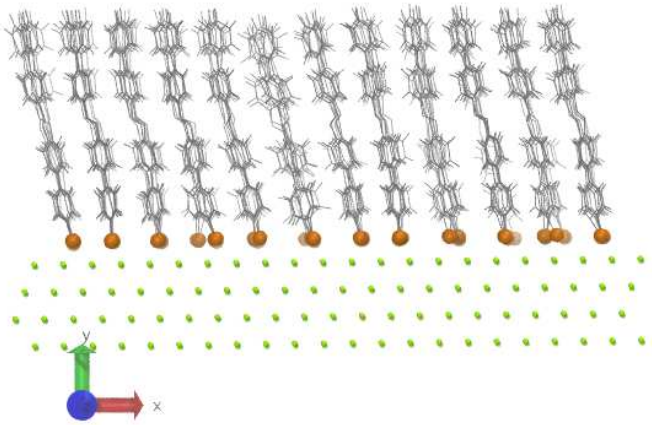

Figure S2: Snapshot of the unit cell of the all-*cis* SAM. The Au atoms of the upper layer are shown as small dots, the S atoms as larger yellow circles. Left panel: side view. Right panel: top view. In the latter case, the lower phenyl rings are in blue, the azobenzene moieties in green and the upper phenyl rings in purple.

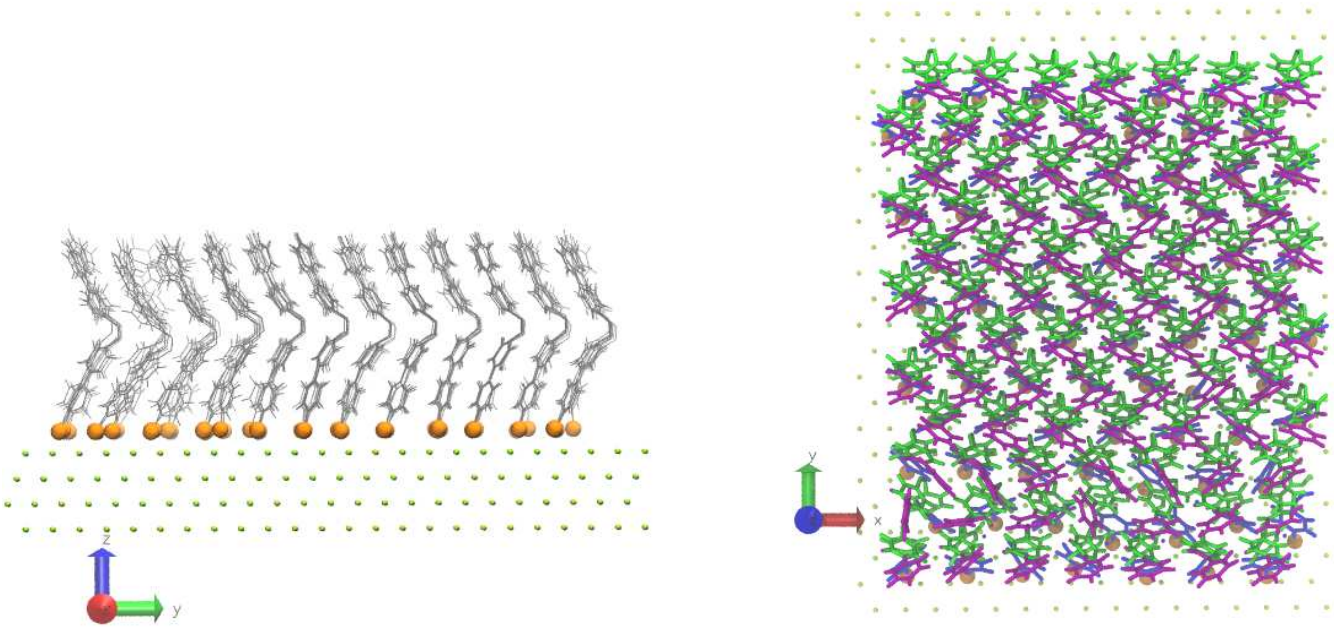

Figure S3: Distributions of the tilt angle θ for the rows of the all-*trans* SAM. The distributions are built as histograms taking account all molecules in each row and all time steps of the MD simulation starting from $t = 4$ ns. The numbering of the rows is the same as in Fig. 2.

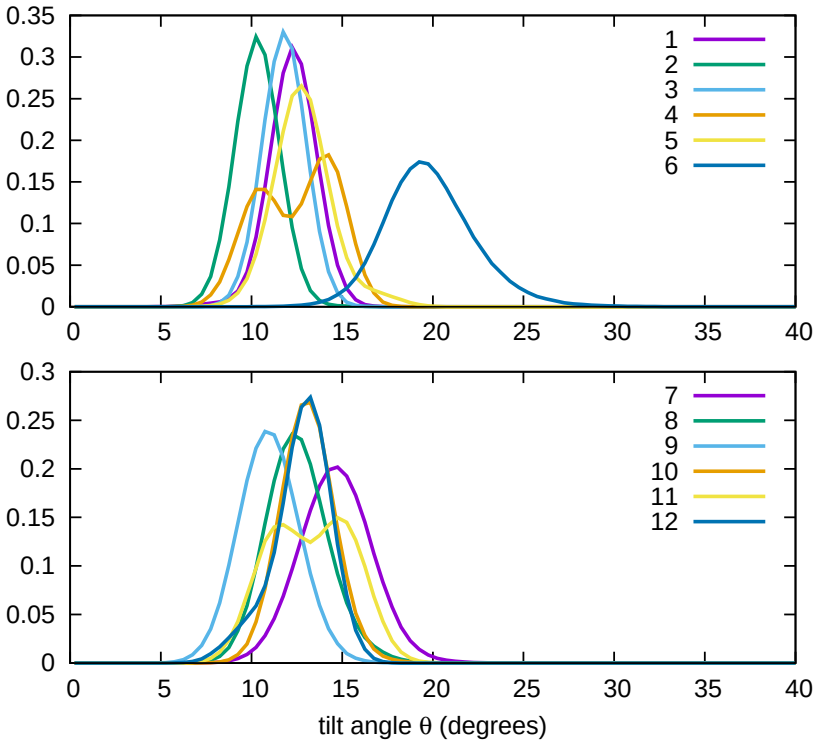

Figure S4: Distributions of the tilt orientation angle ϕ for the rows of the all-*trans* SAM. The distributions are built as histograms taking account all molecules in each row and all time steps of the MD simulation starting from $t = 4$ ns. The numbering of the rows is the same as in Fig. 2.

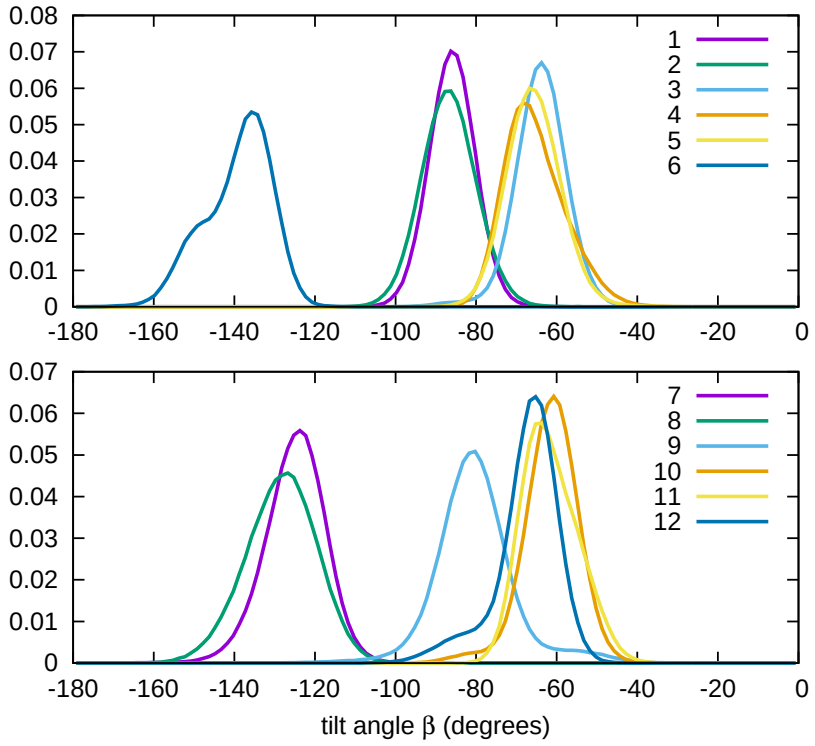

Figure S5: Electronic energy difference (eV) between S_1 and S_0 versus CNNC dihedral (degrees) at hopping points. Excited ABPT molecule in row 6. Positive values of the energy difference for $S_1 \rightarrow S_0$ hops and negative values for backward $S_0 \rightarrow S_1$ hops. Green: reactive (i.e. isomerizing) trajectories. Red: trajectories not giving rise to isomerization.

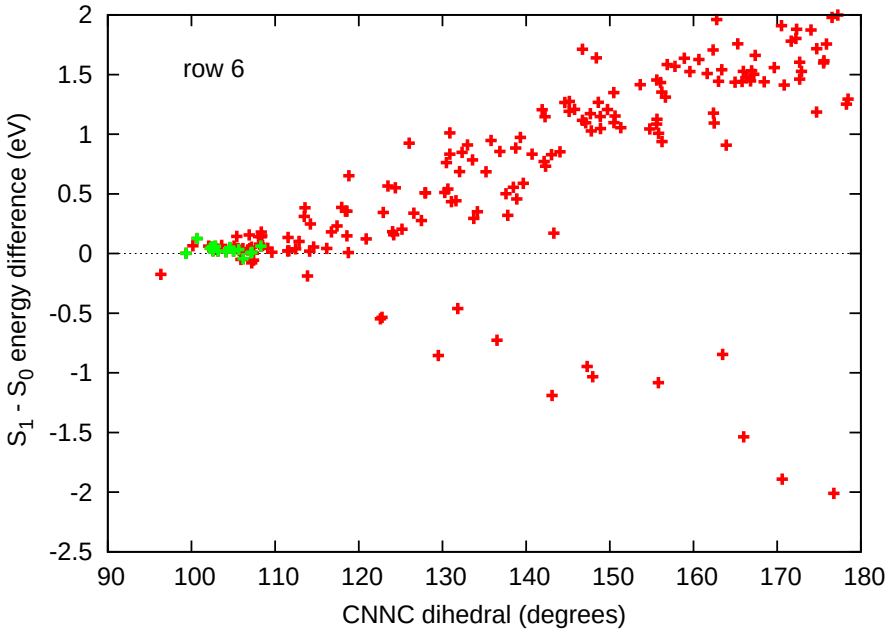

Figure S6: Electronic energy difference (eV) between S_1 and S_0 versus CNNC dihedral (degrees) at hopping points. Excited ABPT molecule in row 3, 4 or 5. Positive values of the energy difference for $S_1 \rightarrow S_0$ hops and negative values for backward $S_0 \rightarrow S_1$ hops.

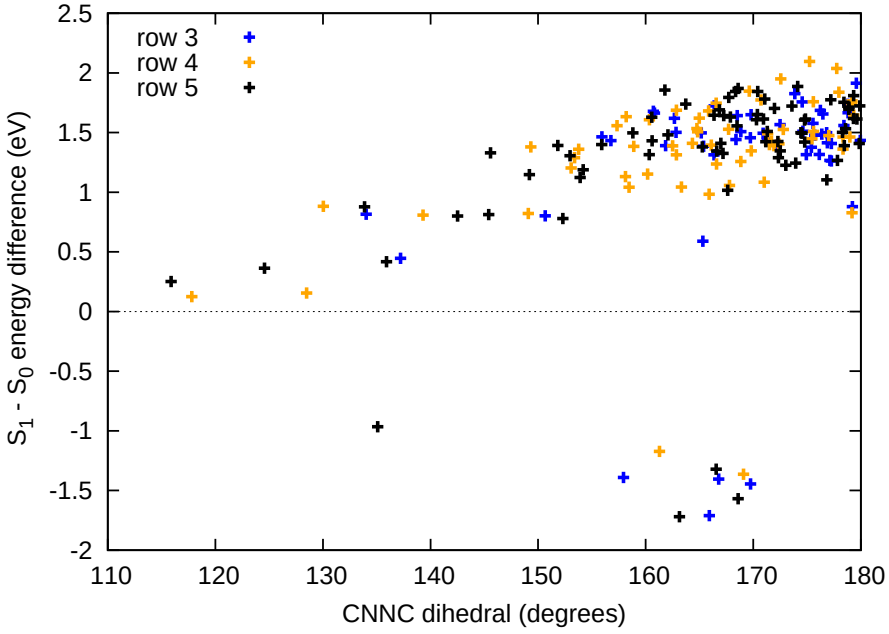

References

[1] Jorgensen, W. L.; Maxwell, D. S.; Tirado-Rives, J. Development and Testing of the OPLS All-Atom Force Field on Conformational Energetics and Properties of Organic Liquids. *J. Am. Chem. Soc.* **1996**, *117*, 11225-11236.

[2] J. W. Ponder, TINKER 6.1, Washington University, San Louis, USA.

[3] Pipolo, S.; Benassi, E.; Brancolini, G.; Valášek, M.; Mayor, M.; Corni, S. First-Principle-Based MD Description of Azobenzene Molecular Rods. *Theor. Chem. Acc.* **2012**, *131*, 1274-1283.

[4] Schapotschnikow, P.; Pool, R.; Vlugt, T. J. H. Selective Adsorption of Alkyl Thiols on Gold in Different Geometries. *Comput. Phys. Commun.* **2007**, *177*, 154-157.

[5] Leng, Y.; Keffer, D. J.; Cummings, P. T. Structure and Dynamics of a Benzenedithiol Monolayer on a Au(111) Surface. *J. Phys. Chem. B* **2003**, *107*, 11940-11950.

[6] J. J. P. Stewart, MOPAC 2002, Fujitsu Limited, Tokio, Japan.

[7] Cusati, T.; Granucci, G.; Martínez-Núñez, E.; Martini, F.; Persico, M.; Vázquez, S. Semiempirical Hamiltonian for Simulation of Azobenzene Photochemistry. *J. Phys. Chem. A* **2012**, *116*, 98-110.

[8] Pace, G.; Ferri, V.; Grave, C.; Elbing, M.; von Hänisch, C.; Zharnikov, M.; Mayor, M.; Rampi, M. A.; Samorì, P. Cooperative Light-Induced Molecular Movements of Highly Ordered Azobenzene Self-Assembled Monolayers. *Proc. Natl. Acad. Sci. USA* **2007**, *104*, 9937-9942.

[9] Tirosh, E.; Benassi, E.; Pipolo, S.; Mayor, M.; Valášek, M.; Frydman, V.; Corni, S.; Cohen, S. R. Direct Monitoring of Opto-Mechanical Switching of Self-Assembled Monolayer Films Containing the Azobenzene Group. *Beilstein J. Nanotechnol.* **2011**, *2*, 834-844.

[10] Antes, I.; Thiel, W. Adjusted Connection Atoms for Combined Quantum Mechanical and Molecular Mechanical Methods. *J. Phys. Chem. A* **1999**, *103*, 9290.

[11] Ciminelli, C.; Granucci, G.; Persico, M. Are Azobenzenophanes Rotation-Restricted? *J. Chem. Phys.* **2005**, *123*, 174317.

[12] Bussi, G.; Parrinello, M. Stochastic Thermostats: Comparison of Local and Global Schemes. *Comp. Phys. Comm.* **2008**, *179*, 26.

[13] Granucci, G.; Persico, M.; Zoccante, A. Including Quantum Decoherence in Surface Hopping. *J. Chem. Phys.* **2010**, *133*, 134111.